Automatic diagnosis and control of distributed solid state lighting systems

Dong, Jianfei; van Driel, Willem; Zhang, Guoqi

DOI
10.1364/OE.19.005772

Publication date
2011

Document Version
Final published version

Published in
Optics Express

Automatic diagnosis and control of distributed solid state lighting systems

Jianfei Dong,[1,*] **Willem van Driel,**[1,2] **and Guoqi Zhang**[1,2]

[1]*Delft University of Technology, 2628CD, Delft, the Netherlands*
[2]*Philips Lighting, 5600 JM, Eindhoven, the Netherlands*
[*]*j.dong@tudelft.nl*

Abstract: This paper describes a new design concept of automatically diagnosing and compensating LED degradations in distributed solid state lighting (SSL) systems. A failed LED may significantly reduce the overall illumination level, and destroy the uniform illumination distribution achieved by a nominal system. To our knowledge, an automatic scheme to compensate LED degradations has not yet been seen in the literature, which requires a diagnostic step followed by control reconfigurations. The main challenge in diagnosing LED degradations lies in the usually unsatisfactory observability in a distributed SSL system, because the LED light output is usually not individually measured. In this work, we tackle this difficulty by using pulse width modulated (PWM) drive currents with a unique fundamental frequency assigned to each LED. Signal processing methods are applied in estimating the individual illumination flux of each LED. Statistical tests are developed to diagnose the degradation of LEDs. Duty cycle of the drive current signal to each LED is re-optimized once a fault is detected, in order to compensate the destruction of the uniform illumination pattern by the failed LED.

OCIS codes: (230.3670) Light-emitting diodes; (110.2945) Illumination design; (220.4830) Systems design; (150.5495) Process monitoring and control.

References and links

1. E. Schubert, J. Kim, H. Luo, and J. Xi, "Solid-state lighting a benevolent technology," Rep. Prog. Phys. **69**, 3069-3099 (2006).
2. I. Ashdown, "Solid-state lighting design requires a system-level approach," in "SPIE Newsroom," (2006). http://newsroom.spie.org/x2235.xml?highlight=x531
3. N. Narendran, N.Maliyagoda, A. Bierman, R. Pysar, and M. Overington, "Characterizing white LEDs for general illumination applications," Proc. SPIE **3938**, 240–248 (2000).
4. C. Tsuei, J. Pen, and W. Sun, "Simulating the illuminance and the efficiency of the LED and fluorescent lights used in indoor lighting design," Opt. Express **16**, 18692-18701 (2008).
5. I. Moreno and U. Contreras, "Color distribution from multicolor LED arrays," Opt. Express **15**, 3607-3618 (2007).
6. Z. Qin, K. Wang, F. Chen, X. Luo, and S. Liu, "Analysis of condition for uniform lighting generated by array of light emitting diodes with large view angle," Opt. Express **18**, 17460-17476 (2010).
7. C. Sun, W. Chien, I. Moreno, C. Hsieh, and Y. Lo, "Analysis of the far-field region of LEDs," Opt. Express **17**, 313918-13927 (2009).
8. Y. Ding, X. Liu, Z. Zheng, and P. Gu, "Freeform LED lens for uniform illumination," Opt. Express **16**, 12958-12966 (2008).
9. M. Blanke, M. Kinnaert, J. Lunze, and M. Staroswiecki, *Diagnosis and Fault-Tolerant Control* (Springer Verlag, Heidelberg, 2003).

#140155 - $15.00 USD Received 23 Dec 2010; revised 7 Feb 2011; accepted 7 Feb 2011; published 14 Mar 2011

10. T. Shen, A. Lau, and C. Yu, "Simultaneous and independent multi-parameter monitoring with fault localization for DSP-based coherent communication systems," Opt. Express **18**, 23608-23619 (2010).
11. H. Yang, J. Bergmans, and T. Schenk, "Illumination sensing in LED lighting systems based on frequency-division multiplexing," IEEE Trans. Signal Proc. **57**, 4269 - 4281 (2009).
12. H. Yang, J. Bergmans, T. Schenk, J. Linnartz, and R. Rietman, "An analytical model for the illuminance distribution of a power LED," Opt. Express **16**, 21641-21646 (2008).
13. A. Descombes and W. Guggenbuhl, "Large signal circuit model for LEDs used in optical communication," IEEE Trans. Electron Devices **28**, 395 - 404 (1981).
14. D. Wood, *Optoelectronic Semiconductor Devices* (Prentice Hall, 1994).
15. L. Ljung, *System Identification - Theory for the User* (Prentice Hall, 1987).
16. F. Gustafsson, *Adaptive filtering and change detection* (John Wiley & Sons, 2001).
17. K. Åström and B. Wittenmark, *Computer controlled systems: theory and design* (Prentice Hall, 1984).
18. IEC 62386, *Digital addressable lighting interface* (2007).
19. S. Boyd and L. Vandenberghe, *Convex Optimization* (Cambridge University Press, 2004).
20. Philips Lumileds, LUXEON Rebel Illumination Portfolio–Technical Datasheet DS63, http://www.philipslumileds.com/pdfs/DS63.pdf.

1. Introduction

Solid-state lighting is gaining more and more popularity nowadays. LEDs can now be easily found in hardware stores. This development is attributed to the great benefits of using LEDs [1], namely high efficiency, controllable emission properties with much greater precision, and the consequent huge environmental benefits. According to the calculations in [1], with a 40% market penetration of solid-state lighting technology, one quarter of the electrical energy currently used for lighting in the US can be saved per year. However, since single LEDs cannot provide sufficient luminous flux alone, they are usually grouped together [2–4]. By distributing the illumination task to each LED in the system, the burden on each individual is significantly reduced. Consequently, the life of each LED can be increased [3].

Recent research in the literature mainly focuses on analyzing the illumination distribution of a group of LEDs [4–7]. A group of LEDs are usually required to achieve a uniform illumination pattern [4, 6, 8]. There is hence an urgent need for system-level design of SSL systems [2]. On the other hand, what is still missing in the illumination literature is an integrated scheme of fault diagnosis and reconfiguration of the LEDs to maintain the uniform illumination, in case that some LEDs in the group degrade. For instance, LED degradation can be due to the excessive increase in its junction temperature [2]. Although one may visually inspect a degraded LED in his/her home and replace it with a new one, it is not as straightforward for the LEDs in an office building or for street lighting. The disturbance to a meeting by the replacement of failed LEDs in the meeting room may be quite annoying. Pedestrians may find failed lamps in street. But it is not up to them to replace these lamps. They have to suffer from darkness, until the lighting system is repaired by the concerned authority. This hence motivates us to investigate an automatic diagnosis and reconfiguration scheme for distributed SSL systems.

Fault diagnosis has been widely applied in safety critical systems [9], e.g. aeroplanes. Recently, it has also attracted attention in optical communication applications, e.g. [10]. Briefly speaking, model-based fault diagnosis is a residual generation and evaluation problem. If only a single LED is applied and there is a photosensor measuring its luminous flux, then diagnosing its degradation is relatively easy, since a residual can be readily computed as the difference between the measured and the theoretical luminous flux. However, as long as a group of LEDs are simultaneously implemented, the problem becomes much more complicated. The difficulties are two folds. First, there are usually not as many photosensors as LEDs, because otherwise the cost would be too high. If there is only one photosensor measuring the entire group of LEDs, then its measurement is a mixture of all the LED outputs. It is not easy to separate these signals. Second, even if there are as many photosensors as LEDs, the photosensors may still be influenced by all the LEDs. The separation of these mixed measurements into individual flux

#140155 - $15.00 USD Received 23 Dec 2010; revised 7 Feb 2011; accepted 7 Feb 2011; published 14 Mar 2011

of each LED depends on the invertibility of the mapping from the individuals to the mixtures.

In this research, we solve the observability problem mentioned above by the illumination sensing method proposed in [11]. We consider the case where there are less photosensors than LEDs in a SSL system. Separating the light signals is made possible by tagging the drive current signal to each LED with a distinguishable "identity". In [11], the drive current signal to each LED is assigned with a unique fundamental frequency, which is known as frequency division multiplexing (FDM). As a consequence, it is natural to separate each LED contribution to the overal illumination at the photosensor by a bank of band-pass filters. Based on this "virtual sensing" approach, we will develop in this paper a statistical method to diagnose the degradations of LEDs in a SSL system, and a criteria for determining the number and position of the photosensors to ensure the efficiency of this diagnostic scheme.

Once degradations of some LEDs are detected, an automatic reconfiguration of the drive current signals to the LEDs in the system is required to compensate the destroyed uniform illumination pattern. In this reconfiguration, the failed LEDs should be turned off; and the properly-working LEDs should be given more duty to compensate the loss of the failed LEDs. To this end, we will develop in this paper an optimization-based scheme, and combine it with the diagnostic scheme into an integrated fault tolerant control (FTC) scheme for distributed SSL systems. The condition for efficient compensation will also be analyzed.

The rest of the paper is organized as follows. LED illumination rendering and sensing are briefly reviewed in Sec. 2. A new statistical diagnostic method is developed in Sec. 3, followed by an optimization-based control reconfiguration method to maintain a uniform illumination pattern in Sec. 4. Detailed simulation studies are presented in Sec. 5, which verifies the effectiveness of the proposed scheme. Conclusions will finally be given in Sec. 6.

2. Illumination rendering and sensing of LEDs

Lambertian model is widely used in describing the illumination pattern of LEDs [4–6, 12]. The illuminance, i.e. the luminous flux per unit area, at a target point on a flat surface with a horizontal and vertical distance of respectively d and h from a single LED can be expressed by the following Lambertian model [12],

$$\ell(d,h) = \frac{(\mu+1)\ell_0}{2\pi h^2}\left(1+\frac{d^2}{h^2}\right)^{-\frac{\mu+3}{2}}. \tag{1}$$

Here, $\ell(d,h)$ denotes the illuminance in the unit of lumen/m^2. ℓ_0 is the total luminous flux (in lumen) produced by the LED. μ (>0) is the Lambertian mode number, dependent on the view angle at which the illuminance is half of the value at $\theta = 0$ [5, 12]. The geometry is illustrated in Fig. 1.

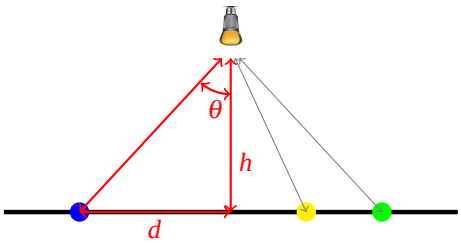

Fig. 1. Geometry between an LED and a target. Circles: target points.

#140155 - $15.00 USD Received 23 Dec 2010; revised 7 Feb 2011; accepted 7 Feb 2011; published 14 Mar 2011

The overall illumination rendered by a group of LEDs, as shown in Fig. 2, is a superposition of all the individual Lambertian model outputs. In order to separate these outputs, frequency

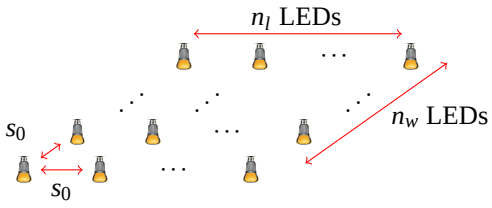

Fig. 2. An $n_l \times n_w$ LED array on a flat surface with equal spacing s_0.

division multiplexing scheme is applied to pulse width modulated (FDM-PWM) drive current signals in [11]. The FDM-PWM drive current pulses lead to light pulses as illustrated in Fig. 3, where f_i is the fundamental frequency of the drive current fed to the i-th LED; $0 < p_i < 1$ is the length of one duty cycle.

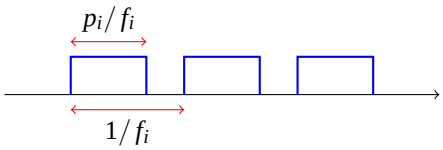

Fig. 3. FDM-PWM light pulses.

The light pulse shape of an LED in response to one period of the FDM-PWM drive current signal can be written as [11, 13]

$$q_i(t) = \begin{cases} 0, & t \le -\frac{p_i}{2f_i} \\ 1 - e^{-\frac{t+\frac{p_i}{2f_i}}{\tau_{on,i}}}, & -\frac{p_i}{2f_i} \le t \le \frac{p_i}{2f_i} \\ \left(1 - e^{-\frac{p_i}{f_i \tau_{on,i}}}\right) \cdot e^{-\frac{t+\frac{p_i}{2f_i}}{\tau_{off,i}}}, & t \ge \frac{p_i}{2f_i} \end{cases} . \tag{2}$$

To avoid flicker and to ignore the transient response of the LEDs to the drive current, the fundamental frequencies should be chosen within the band $2kHz \le f_i \le 4kHz, \forall i$ [11]. Hence, if $\frac{p_i}{f_i} \gg \tau_{on,i}, \tau_{off,i}$, the function $q_i(t)$ can be well approximated by $rect\left(\frac{tf_i}{p_i}\right)$. Here, $rect(t)$ is a rectangular function, i.e.

$$rect(t) = \begin{cases} 1, & -\frac{1}{2} \le t \le \frac{1}{2} \\ 0, & otherwise \end{cases} . \tag{3}$$

$\tau_{on,i}$ and $\tau_{off,i}$ are the time constant of the i-th LED of respectively on and off switch. Usually, $\tau_{on,i} + \tau_{off,i} \le 250ns$ [11].

The overall illumination from L LEDs measured by the photosensor, at the position of (x,y,h), can be expressed as

$$I_{x,y,h}(t) = \sum_{i=1}^{L} \sum_{n=-\infty}^{\infty} a_{f,i} \cdot q_i\left(t - \frac{n}{f_i}\right) + e(t). \tag{4}$$

#140155 - $15.00 USD Received 23 Dec 2010; revised 7 Feb 2011; accepted 7 Feb 2011; published 14 Mar 2011

Here, $a_{f,i} = \alpha_i \cdot \ell_i(x,y,h)$, with α_i standing for the gain from the i-th LED to the illumination measured by the photosensor. $\ell_i(x,y,h)$ is the Lambertian model output of the i-th LED at the position of the photosensor, with (x,y) the coordinates on the target surface; i.e. $d = \sqrt{x^2+y^2}$. The last term $e(t)$ consists of thermal and shot noise in the photosensor circuit, which is usually considered as zero mean white Gaussian in literature [11]. Here, we also assume that there is no ambient light, except the LEDs in the SSL system.

The task of illumination sensing is therefore to estimate $a_{f,i}$ for each individual LED. At each fundamental frequency f_i, $a_{f,i}$ can be estimated by

$$\hat{a}_{f,i}(t) = \frac{\pi}{\sin(\pi p_i)} \cdot \left| \int_0^T I_{x,y,h}(t-\tau) \cdot g(\tau) \cdot e^{-j2\pi f_i \tau} \cdot d\tau \right|. \tag{5}$$

Here, $g(t)$ represents the impulse response parameters of a filter defined on the support $[0,T]$. In [11], to achieve unbiased illumination sensing, $g(t)$ is taken as

$$g(t) = \frac{1}{T} \cdot rect\left(\frac{t}{T} - \frac{1}{2}\right), \tag{6}$$

where $T \geq \frac{1}{\Delta_f}$, with $\Delta_f = \frac{f_{upper} - f_{lower}}{L}$, with f_{upper}, f_{lower} respectively the upper and lower frequency limit. Note that the estimate, $\hat{a}_{f,i}$, is a function of time now, because it is the output from a dynamic filter. Furthermore, due to the measurement noise $e(t)$, the estimation error is upper bounded as [11]

$$|a_{f,i}(t) - \hat{a}_{f,i}(t)| \leq |v_i(t)|, \tag{7}$$

where $v_i(t)$ has a variance of

$$P_e \cdot \int_{-\infty}^{\infty} g^2(t)dt = \frac{P_e}{T}, \tag{8}$$

with P_e the double-sided power spectrum density of $e(t)$.

The illumination sensing scheme can now be illustrated as in Fig. 4.

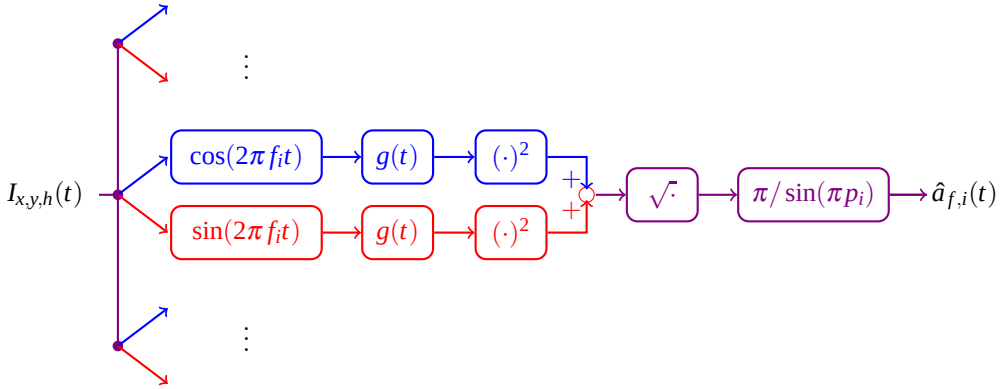

Fig. 4. Filter bank for illumination sensing using FDM-PWM drive current signals with a unique fundamental frequency to each LED.

3. Diagnosis of LED degradations

3.1. *Diagnostic method*

In this paper, we consider the degradation of an LED as the reduction in its efficiency from drive current to its light output. Briefly speaking, fault diagnosis is a residual generation and

#140155 - $15.00 USD Received 23 Dec 2010; revised 7 Feb 2011; accepted 7 Feb 2011; published 14 Mar 2011

evaluation problem. We shall treat the estimated illumination via the method introduced in the previous section as measured signals, and compare them with its theoretical counterparts.

The light output from an LED is known to be proportional to the drive current flowing through it at steady state [13, 14]. Besides, the dynamic response of light output to drive current has a first-order behavior with the on-/off-switching time constant of the LED. The transient response can hence be neglected as discussed in Sec. 2. The following equalities hold.

$$\ell_{0,i}(t) = \eta_i \cdot c_i(t). \tag{9}$$

$$a_{f,i}(t) = \eta_i \cdot \underbrace{c_i(t) \cdot \alpha_i \cdot \frac{\mu_i+1}{2\pi h^2} \cdot \left(1+\frac{d_i^2}{h^2}\right)^{-\frac{\mu_i+3}{2}}}_{\psi_i(t)}. \tag{10}$$

Here, c_i is the amplitude of drive current pulses flowing through the i-th LED. η_i is the responsivity coefficient. In addition to the theoretical relation $\ell_{0,i} = \eta_i \cdot c_i$, $\ell_{0,i}$ can also be found by interpolating the current versus luminous flux chart provided on the data sheet of an LED, e.g. [20]. In this case, $\eta_i \cdot c_i$ in Eq. (10) (and Eq. (17) later in this paper) can be replaced by the interpolated values according to the data sheet. Besides, we shall treat the nominal values of α_i, η_i, μ_i as known parameters. Note also that if α_i, η_i, μ_i are unknown, they can instead be identified from data, by standard parameter fitting or system identification techniques, e.g. those in [15]. The theoretical value of $a_{f,i}(t)$ can hence be calculated.

The residual can now be written as

$$r_i(t) = a_{f,i}(t) - \hat{a}_{f,i}(t), \tag{11}$$

where $\hat{a}_{f,i}(t)$ is from the "virtual sensor", i.e. (5), realized by the i-th channel of the filter bank illustrated in Fig. 4. The components of $r_i(t)$ include a random noise (denoted by w_i), whose distribution is determined by (7), and in the faulty case, a fault signal (denoted by φ_i); i.e.

$$r_i(t) = \varphi_i(t) + w_i(t). \tag{12}$$

For fault diagnosis, φ_i needs not be to known or modeled. However, it is relevant to see how φ_i is related to the degradation of the i-th LED. For instance, suppose the responsivity of the i-th LED is reduced by a factor to $\eta_i' = \delta \cdot \eta_i$, with $0 \le \delta \le 1$. But the estimate, $\hat{a}_{f,i}(t) = \eta_i' \psi_i(t) + w_i(t)$, faithfully reflects the degraded illumination up to the random error $w_i(t)$. Hence, the signal $\varphi_i(t)$ takes care of the change in the mean; i.e.

$$\varphi_i(t) = \eta_i \psi_i(t) - \eta_i' \psi_i(t) = (1-\delta) \cdot \eta_i \cdot \psi_i(t). \tag{13}$$

On the other hand, the complete breakdown of the i-th LED can be modeled by taking $\delta = 0$.

We can now analyze the statistical characteristics of $r_i(t)$ due to the noise term w_i, and develop a fault diagnosis test. In fact, due to (7),

$$\left| \frac{a_{f,i}(t) - \hat{a}_{f,i}(t)}{\sqrt{P_e/T}} \right| \le \left| \frac{v_i(t)}{\sqrt{P_e/T}} \right| \Leftrightarrow \frac{\left[a_{f,i}(t) - \hat{a}_{f,i}(t)\right]^2}{P_e/T} \le \frac{v_i^2(t)}{P_e/T}. \tag{14}$$

Since $v_i(t)$ is zero mean Gaussian with variance P_e/T, the random variable $\frac{v_i^2(t)}{P_e/T}$ is χ^2 distributed with a DoF of 1 [16], denoted as χ_1^2. In other words, the random variable $\boldsymbol{\zeta}_i(t) \triangleq \frac{\left[a_{f,i}(t) - \hat{a}_{f,i}(t)\right]^2}{P_e/T}$ is upper bounded by the χ_1^2 distributed variable $\boldsymbol{\nu}_i(t) \triangleq \frac{v_i^2(t)}{P_e/T}$. This then leads to a fault diagnosis

#140155 - $15.00 USD Received 23 Dec 2010; revised 7 Feb 2011; accepted 7 Feb 2011; published 14 Mar 2011

test in terms of the worst case estimation error; i.e.

$$\boldsymbol{\zeta}_i(t) \underset{\text{no fault}}{\overset{\text{faulty}}{\gtrless}} \gamma_{\chi_1^2,\beta} \tag{15}$$

where $\gamma_{\chi_1^2,\beta}$ denotes the threshold, determined by a chosen false alarm rate β.

Note that the threshold $\gamma_{\chi_1^2,\beta}$ is determined by $\boldsymbol{\nu}_i(t)$, i.e. the upper bound of $\boldsymbol{\zeta}_i(t)$. If $\boldsymbol{\nu}_i(t)$ stays below this threshold, then so does $\boldsymbol{\zeta}_i(t)$. In other words, $\boldsymbol{\zeta}_i(t)$ is less probable to exceed $\gamma_{\chi_1^2,\beta}$ than $\boldsymbol{\nu}_i(t)$ is with probability β, when the i-th LED works properly. This is to say that the test (15) is robust to the worst-case estimation error, but at the price of being more conservative.

3.2. Placement of photosensors for efficient diagnosis

The diagnostic method proposed in this paper relies on the estimated illumination by a photosensor. One question to answer now is whether one photosensor suffices in monitoring an entire array of LEDs. Intuitively, the answer depends on how well the photosensor can see each LED in the array. Technically, the number and positions of the photosensors shall be determined by the signal-to-noise ratio (SNR) of the luminous flux of the i-th LED $a_{f,i}(t)$ to the estimation error $v_i(t)$, as defined in (7); i.e. $SNR_i = \frac{a_{f,i}^2(t)}{P_e/T}$.

On the other hand, $a_{f,i}(t) = \alpha_i \cdot \ell_i(x,y,h)$ is determined by the relative position (or the solid angle θ, see Fig. 1) between the i-th LED and the photosensor and the Lambertian mode number of the LED, i.e. μ_i. For a narrow Lambertian-type LED, μ_i is big, leading to fast decaying luminous flux as the solid angle θ increases. In this case, a photosensor should be placed at small solid angles relative to the LEDs, which is thus limited to monitor the LEDs only in its close neighborhood. Conversely, when μ_i is small, one photosensor is able to effectively monitor more LEDs further away from its neighborhood.

The SNR determines the sensitivity of the diagnostic method. For the complete failure of an LED, the mean of the estimate, $\hat{a}_{f,i}(t)$, becomes zero, since there is no more light output from this LED. Whereas, based on the nominal parameters, $a_{f,i}(t)$ still reflects the nominal luminous flux. The mean of the residual, $r_i(t)$, hence reaches its maximum, i.e. $a_{f,i}(t)$. The test statistic then equals $\frac{[a_{f,i}(t)+w_i(t)]^2}{P_e/T}$. Here, $w_i(t)$ is stochastic. With a probability of 0.5, $w_i(t) > 0$. This indicates that within a few consecutive sampling instants, there is at least one $w_i(t)$ almost surely positive. In other words, if the SNR satisfies the following condition,

$$SNR_i = \frac{a_{f,i}^2(t)}{P_e/T} > \gamma_{\chi_1^2,\beta}; \tag{16}$$

then the fault is almost surely detectable within a few consecutive samples, since $[a_{f,i}(t) + w_i(t)]^2 > a_{f,i}^2(t)$ almost surely within this short interval. This condition can be used to determine the number and positions of the photosensors to efficiently diagnose LED degradations.

4. Control reconfiguration against LED degradations

The desired performance of a SSL system is the uniformly distributed illumination on a target surface with a certain intensity. If this performance is achieved by the nominal system, then a degraded LED will destroy this uniformity, and especially reduce the illumination around it. Therefore, it is necessary to compensate this degradation by the other nominal LEDs in the system. This can be done by automatically tuning the (average) amplitudes of the drive current fed into these nominal LEDs, once the degradation of an LED is detected. To this end, we intend to develop an optimization-based scheme in this section.

#140155 - $15.00 USD Received 23 Dec 2010; revised 7 Feb 2011; accepted 7 Feb 2011; published 14 Mar 2011

4.1. Optimization-based control reconfiguration

Due to the rectangular LED light pulses in response to the PWM drive current signals, the average flux of the i-th LED in one period is the total luminous flux produced by the peak current c_i scaled by the on/off switching ratio (i.e. the duty cycle), p_i. At a point (x,y,h) on the target surface, the average illuminance can be written as

$$\mathscr{I}_{x,y,h} = \sum_{i=1}^{L} p_i \cdot \eta_i \cdot c_i \cdot \underbrace{\alpha_i' \cdot \frac{\mu_i+1}{2\pi h^2} \cdot \left(1+\frac{d_i^2}{h^2}\right)^{-\frac{\mu_i+3}{2}}}. \tag{17}$$

Here, α_i' is the path loss of the free-space optical channel from the i-th LED to the target. Note that we use a different notation for the illuminance from that used in (5), since the illuminance defined in (17) needs to be computed, instead of being measured. Note also that the underbraced term in (17) has a fixed value, once the LED array is mounted. To be used in the cost function of the optimization problem later, $\mathscr{I}_{x,y,h}$ quantities the illumination distribution at a target point.

Now, suppose that the i-th LED has degraded, i.e. $\eta_i' < \eta_{i,nominal}$. To still maintain a uniform illumination distribution, it is not efficient and may even not be possible to increase p_i ($0 < p_i < 1$) such that $p_i' \cdot \eta_i' = p_i \cdot \eta_{i,nominal}$. Instead, we intend to compensate the degraded LED with the remaining properly-working LEDs. The degraded one will be switched off. We can hence set the duty cycle p_i to zero in (17) corresponding to the degraded LED, to turn it off.

The deviation of the illuminance from a reference, denoted by $\mathscr{R}_{x,y,h}$, can be quantified as

$$\sum_{(x,y)\in\mathbf{TS}} \left(\mathscr{I}_{x,y,h} - \mathscr{R}_{x,y,h}\right)^2. \tag{18}$$

Here, "**TS**" denotes the target surface. In practice, one can take the reference $\mathscr{R}_{x,y,h}$ to be the same as the original illuminance with all LEDs in the system working properly.

In optimal control [17], cost functions usually contain not only the tracking error cost (18), but also a penalization term on control signals, since the power consumption of the control system also has to be minimized. The following cost function is thus formulated.

$$\mathscr{J} = \sum_{(x,y)\in\mathbf{TS}} w_{(x,y)} \cdot \left(\mathscr{I}_{x,y,h} - \mathscr{R}_{x,y,h}\right)^2 + \sum_{i\in\boldsymbol{I}_{all}\backslash\boldsymbol{I}_{fail}} w_{p_i} \cdot p_i^2. \tag{19}$$

Here, $w_{(x,y)} \geq 0, (x,y) \in \mathbf{TS}$ and $w_{p_i} \geq 0, i \in \boldsymbol{I}_{all}\backslash\boldsymbol{I}_{fail}$ are weighting coefficients respectively penalizing the tracking errors and duty cycles. The set $\boldsymbol{I}_{all} = \{1,\cdots,L\}$ collects all the LED indices in the SSL system; while $\boldsymbol{I}_{fail}$ only contains the indices of the failed LEDs. The set, $\boldsymbol{I}_{all}\backslash\boldsymbol{I}_{fail}$, hence refers to all the remaining properly working LEDs in the system.

By its definition, the duty cycle p_i has to be limited between 0 and 1. More precisely, in an FDM scheme [11, 18], p_i is required to be within the range, $0.001 \leq p_i \leq 0.97307$. The upper bound is to distinguish the current signals from DC. The cost (19), together with these bounds, leads to the following constrained optimization problem.

$$\begin{array}{ll} & \min_{\{p_i | i\in\boldsymbol{I}_{all}\backslash\boldsymbol{I}_{fail}\}} \mathscr{J} \\ s.t. & 0.001 \leq p_i \leq 0.97307, i \in \boldsymbol{I}_{all}\backslash\boldsymbol{I}_{fail} \end{array}. \tag{20}$$

Note that since p_i is linear in $\mathscr{I}_{x,y,h}$, $\mathscr{J}$ is quadratic and convex. Therefore, (20) is a convex optimization problem with global minimum [19].

4.2. Limits in the control reconfiguration

The reconfiguration depends on the redundancy of LEDs. Here, "redundancy" refers not only to the number of LEDs, but also to the superposition of the light outputs from a number of

#140155 - $15.00 USD Received 23 Dec 2010; revised 7 Feb 2011; accepted 7 Feb 2011; published 14 Mar 2011

LEDs at a target point. Besides, a failed LED mostly reduces the illuminance at the point at a zero solid angle with it. A sufficient condition to achieve the same illuminance at such a point can therefore be written as

$$\sum_{i\in \boldsymbol{I}_{an}} 0.97307\cdot \eta_i c_i \alpha_i' \frac{\mu_i+1}{2\pi h^2}\left(1+\frac{d_i^2}{h^2}\right)^{-\frac{\mu_i+3}{2}} \geq \sum_{i\in \boldsymbol{I}_{an}\cup \boldsymbol{I}_{fail}} p_i\cdot \eta_i c_i \alpha_i' \frac{\mu_i+1}{2\pi h^2}\left(1+\frac{d_i^2}{h^2}\right)^{-\frac{\mu_i+3}{2}}; \tag{21}$$

i.e. if the adjacent neighbors (whose indices are denoted by $\boldsymbol{I}_{an}$) of the failed LEDs work at the maximum duty cycle ($p_i = 0.97307, i\in \boldsymbol{I}_{an}$), then the achieved total illuminance at a target point should be greater than or equal to the original total illuminance achieved by these neighbors together with the latterly failed LEDs, at their nominal duty cycles, $p_i, i\in \boldsymbol{I}_{an}\cup \boldsymbol{I}_{fail}$.

If (21) is not satisfied, then the optimization scheme (20) cannot guarantee that the same illuminance at an arbitrary target point is maintained, when a nearby (in terms of solid angle) LED fails, by tuning the duty cycles of the properly-working LEDs. In this case, the failed LEDs should be replaced by new ones as soon as their failure is alerted by the diagnostic scheme.

(21) implies that for efficient reconfiguration, the nominal duty cycles of LEDs should be set below the maximum, 0.97307. Besides, it is easier to satisfy (21); when one LED fails, but its adjacent LEDs do not. To deal with the case that two or more adjacent LEDs fail at the same time, (21) may lead to a conservative choice of nominal duty cycles and more densely placed LEDs. It is hence not realistic to consider adjacent LED failures when using (21) to design the nominal duty cycles and LED spacing. But nonadjacent multiple LED failures are allowed.

4.3. Integrated diagnosis and control reconfiguration

With both the diagnostic method developed in Sec. 3 and the control reconfiguration approach in Sec. 4.1, an integrated fault tolerant control (FTC) scheme for distributed SSL systems is summarized in Alg. 1, and schematically illustrated in Fig. 5.

Algorithm 1 (FTC of a SSL system)

Parameters: *the set of all the LED indices, i.e.* $\boldsymbol{I}_{all}$*; nominal parameter values of the i-th LED, i.e.* $\eta_i, \alpha_i', p_i, \mu_i, f_i, x_i, y_i$*; peak of drive current,* c_i*; photosensor position and parameters,* α_i, P_e*; rectangular filter window length,* T*; detection threshold,* $\gamma_{\chi_1^2,\beta}$*; coordinates of the discrete grid on the target surface; reference illuminance* $\mathscr{R}_{x,y,h}$ *on the target surface; weighting coefficients,* $w_{(x,y)}, w_{p_i}$.

At time instant t**, do the following**:

1. *Read the measurement of the photosensor, i.e.* $I_{x,y,h}(t)$.
2. *Estimate* $a_{f,i}(t)$ *by* (5) *for each LED in the array.*
3. *Compute the statistic* $\frac{\left[a_{f,i}(t)-\hat{a}_{f,i}(t)\right]^2}{P_e/T}$ *and test the hypothesis* (15).
4. *If no degradation is found, return to Step 1; otherwise, record the indices of the failed LEDs in the set* $\boldsymbol{I}_{fail}$*, turn the failed LEDs off, and then continue the following steps.*
5. *Set the weights,* $w_{p_i}, i\in \boldsymbol{I}_{all}\backslash \boldsymbol{I}_{fail}$*, corresponding to the duty cycles of the properly-working LEDs in the close neighborhood the failed ones to zero, to allow them sufficiently increase below the upper bound.*
6. *Solve the optimization problem* (20) *for* $p_i, \forall i\in \boldsymbol{I}_{all}\backslash \boldsymbol{I}_{fail}$.

Outputs: *Alarms and reconfigured duty cycles of the drive current to the nominal LEDs.*

#140155 - $15.00 USD Received 23 Dec 2010; revised 7 Feb 2011; accepted 7 Feb 2011; published 14 Mar 2011

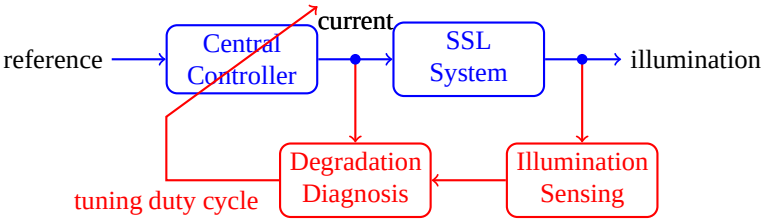

Fig. 5. Scheme of fault tolerant control of a SSL system.

5. Application case study

Consider a 9×9 LED array on a $2m \times 2m$ flat surface, as shown in Fig. 2. Consider the following numerical values: $\mu_i = 50, s_0 = 0.25m$ and $\ell_{0,i} = 100$ lumens at $c_i = 350$mA, i.e. $\eta_i = 285.7$lumen/A, $i = 1, \cdots, 81$. This can be realized by a LUXEON Rebel LXM7-PW40 LED [20]. The optical channel gains are set as $\alpha = 1, \alpha' = 1$. P_e is chosen as 0.01.

Suppose there is only one photosensor on the target surface, two meters below the LED array. Its position on the surface is $(0.3, 0.3)m$, with the origin fixed at the central LED of the array. We shall use this sensor to estimate $a_{f,i}, i = 1, \cdots, 81$. The contribution of each individual LED to the photosensor is illustrated in Fig. 6.(a), where the gray levels are calculated as

$$0.97 \cdot \left(1 - \frac{a_{f,i}}{a_{f,max}} \cdot [1\ 1\ 1]\right), \quad i = 1, \cdots, 81, \tag{22}$$

with $a_{f,max} = \max\{a_{f,i} | i = 1, \cdots, 81\}$. The vector, $[1\ 1\ 1]$, represents normalized RGB values. The more visible (the darker) the circles are seen by the readers, the more visible the LEDs are to the photosensor. On the other hand, Fig. 6.(b) indicates that the majority of the LEDs contributes to an SNR greater than $10dB$, sufficient for diagnosing degradations. We shall hence only use this photosensor in this paper.

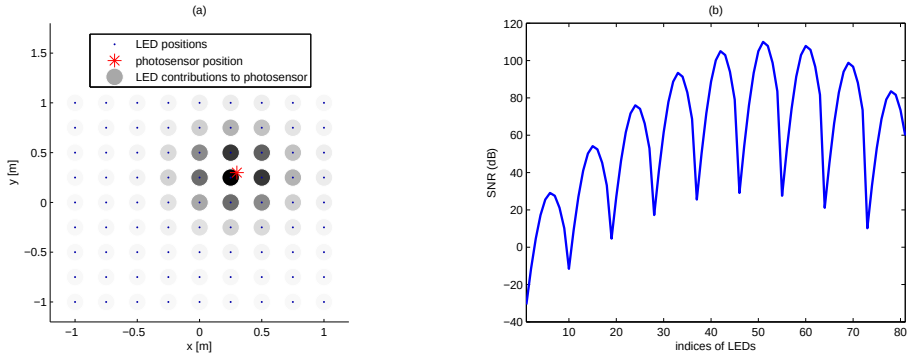

Fig. 6. Contributions of the LEDs to the photosensor. (a). Spatial pattern. (b). SNRs.

The frequency spacing of the FDM-PWM drive current signals is therefore $\Delta_f = \frac{f_{upper} - f_{lower}}{L} = 24.7Hz$. The rectangular filter window is hence chosen to be $T = 0.0405sec$. The initial duty cycles to all the LEDs in the array are chosen as, $p_i = 0.4, \forall i$. The sampling

#140155 - $15.00 USD Received 23 Dec 2010; revised 7 Feb 2011; accepted 7 Feb 2011; published 14 Mar 2011

period is set to 10^{-6} seconds. The target surface is discretized with a spacing of 0.01m into a 201×201 grid.

Suppose the LEDs have been running for 10^5 hours. Consider the fault of the central LED, with the efficiency degraded to 20%. This degradation is injected into the LED at $0.075sec$ after 10^5 hours. The other LEDs are not changed. With this degradation, the overall illumination pattern is shown in Fig. 7. It can be seen that the area adjacent to the projected point of the degraded LED becomes dimmer. The uniformity in the center of the surface is destroyed.

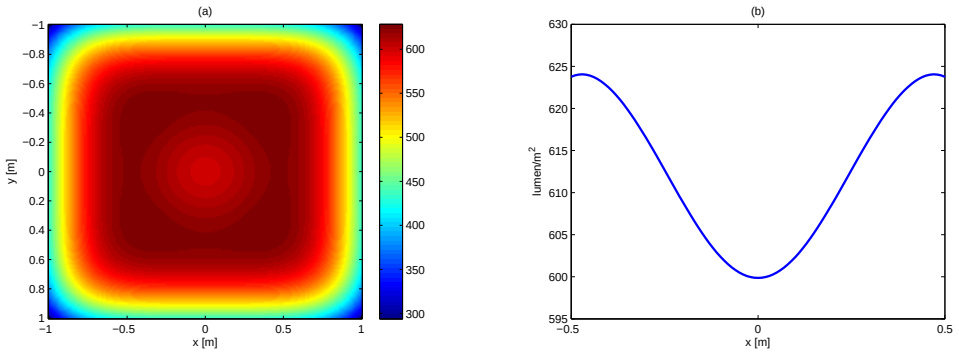

Fig. 7. Illumination distribution (lumen/m^2) of the LED array with a degraded LED in the center. (a). Overall spatial distribution. (b). Distribution along the line of $-0.5 \leq x \leq 0.5, y = 0$.

To automatically correct the destruction of the uniform illumination pattern, we implement the FTC scheme proposed in this paper. The false alarm rate is chosen as $\beta = 1\%$. The threshold is therefore $\gamma_{\chi_1^2,\beta} = 6.6349$, corresponding to an SNR of $8.2dB$. The total simulation time is $0.15sec$.

The test statistics $\boldsymbol{\zeta}_i(t)$ are plotted in Fig. 8. The vertical lines in the figure divide the time axis into four intervals; i.e. $\mathbb{I}_1 = [0, 0.0405], \mathbb{I}_2 = [0.0405, 0.075], \mathbb{I}_3 = [0.075, 0.1155], \mathbb{I}_4 = [0.1155, 0.15]$. This is because the filter window length is $T = 0.0405sec$. In $\mathbb{I}_1$, the filter waits for sufficiently long signal segment to process. There is hence no output from Alg. 1. In $\mathbb{I}_2$, all the LEDs work properly. So the statistics are restrained below the threshold. The central LED degrades at $0.075sec$. In $\mathbb{I}_3$, all the estimated $\hat{a}_{f,i}$ are biased, due to the transient phase of the estimation filter. To see this, note that the filter $g(t)$ is in fact a moving average of the light signals measured during the past $0.0405sec$. In $\mathbb{I}_4$, when the filter window is entirely filled with degradation-affected light signals, the estimated $\hat{a}_{f,i}, \forall i$ become unbiased again, which result in the statistics below the threshold, only except the one corresponding to the degraded LED. A correct alarm and a trigger of the control reconfiguration step are therefore made. The detection delay is hence $T = 0.0405sec$.

For the optimization-based reconfiguration, we choose the reference $\mathscr{R}_{x,y,h}$ to be the same as the original illuminance produced when all the LEDs working properly with $p_i = 0.4$ and $c_i = 350$mA. The weights are set to $w_{(x,y)} = 10, \forall (x,y) \in \mathbf{TS}$, $w_{p_i} = 0$ for the eight nominal LEDs surrounding the center, and $w_{p_i} = 0.1$ for the other nominal LEDs further away from the center. The reconfigured illumination distribution is shown in Fig. 9. The variance of the illuminance (in $(\text{lumen/m}^2)^2$) in the range of a $1m \times 1m$ square on the target surface centered at the degraded LED, defined as (with N_{dp} denoting the number of discretized points on this

#140155 - $15.00 USD Received 23 Dec 2010; revised 7 Feb 2011; accepted 7 Feb 2011; published 14 Mar 2011

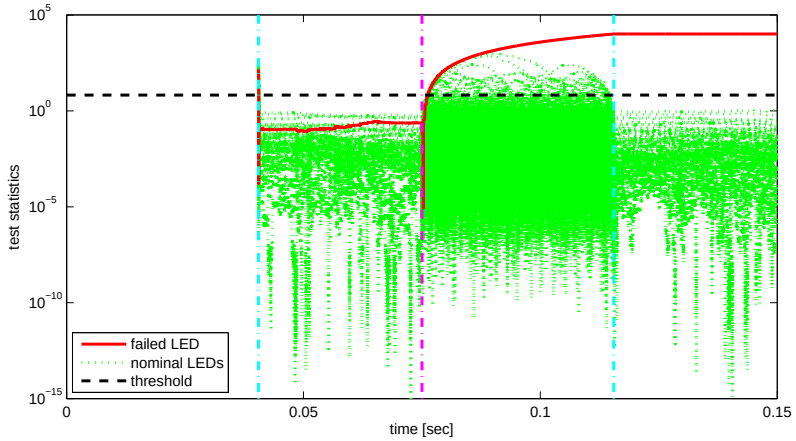

Fig. 8. Test statistics for diagnosing LED degradations. Dash-dotted purple: time instant of the fault onset. Dash-dotted cyan: 0.0405*sec* intervals respectively from the start and from the fault onset.

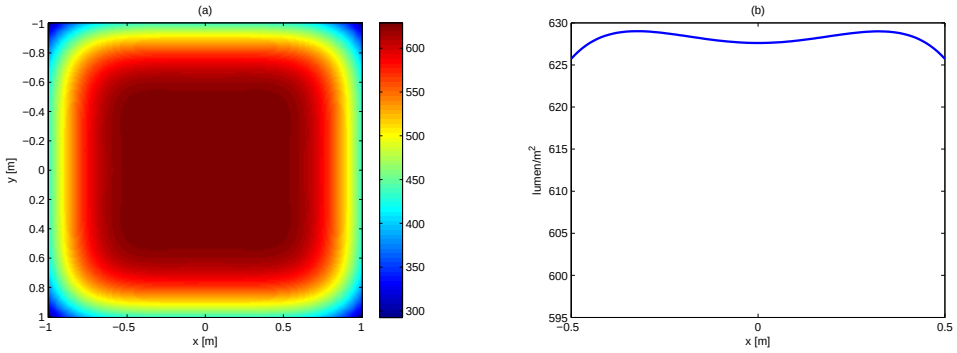

Fig. 9. Reconfigured illumination distribution (lumen/m^2) of the LED array with a degraded LED in the center. (a). Overall spatial distribution. (b). Distribution along the line of $-0.5 \leq x \leq 0.5, y = 0$.

square surface)

$$\frac{1}{N_{dp}} \cdot \sum_{-1 \leq x,y \leq 1} \left(\mathscr{I}_{x,y,h} - \bar{\mathscr{I}}\right)^2, \text{ where } \bar{\mathscr{I}} = \frac{1}{N_{dp}} \cdot \sum_{-1 \leq x,y \leq 1} \mathscr{I}_{x,y,h}, \tag{23}$$

is changed from 56.87 in the degraded case to 0.69 in the reconfigured case; i.e. only 1.22% of the uncompensated value. Clearly, the degraded pattern is efficiently compensated.

It is also interesting to illustrate the reconfigured duty cycles of the LEDs surrounding the degraded one, as in Fig. 10. Obviously, the four nearest LEDs to the degraded one are assigned with longer duty cycles. However, doing so will also increase the illuminance adjacent to these four LEDs. Consequently, the optimization automatically dims the light of their nearest neighbors, in such a way that the uniformity is still maintained as shown in Fig. 9. Moreover, all the reconfigured duty cycles are kept below 0.8, corresponding to an average current of 280*mA*.

#140155 - $15.00 USD Received 23 Dec 2010; revised 7 Feb 2011; accepted 7 Feb 2011; published 14 Mar 2011

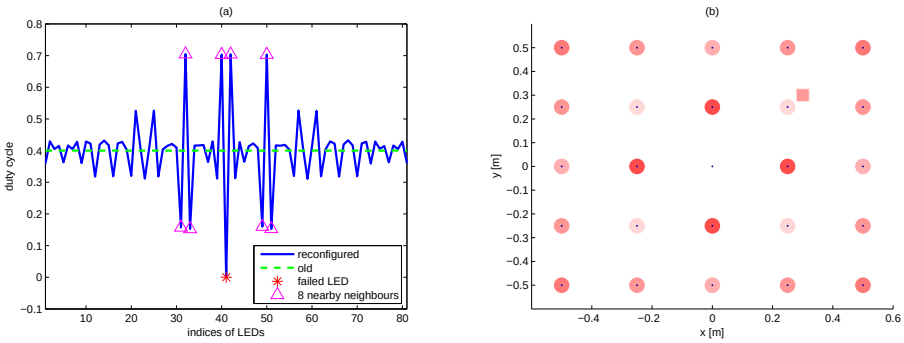

Fig. 10. Reconfigured duty cycles of LED currents. (a). All LEDs. (b). Zoom into the neighborhood of the failed LED. Dots: positions of the LEDs projected onto the target surface. Red square: magnitude of the original duty cycle, $p_i = 0.4, \forall i$. Circles with different levels of red: magnitudes of duty cycles. The darker the circles than the square, the longer their duty cycles than 0.4; and vice versa. The color is calculated as $1 - p_i \cdot [0\ 1\ 1], \forall i$.

6. Conclusions

In this paper, we have developed a new design concept of an automatic fault tolerant control scheme for distributed solid-state lighting systems. The diagnosis of the LED condition in the system is made possible by assigning distinguishable fundamental frequencies to the FDM-PWM drive current signals to all the LEDs. A statistical fault diagnosis approach is proposed based on an illumination sensing method. Optimization-based reconfiguration approach is developed to automatically tune the duty cycles of the FDM-PWM drive current signals. The simulation case study clearly verifies the effectiveness of the proposed FTC scheme. Our future extensions include developing a diagnostic method in the presence of as many photosensors as LEDs, and extending the entire FTC scheme to color LEDs.

Acknowledgement

This study was sponsored by the PrintValley project of Dutch Ministry of Economic Affairs, Agriculture and Innovation.

#140155 - $15.00 USD Received 23 Dec 2010; revised 7 Feb 2011; accepted 7 Feb 2011; published 14 Mar 2011